Scattering from a Semi-Elliptic Channel in a Ground Plane Loaded by a Lossy or Lossless Dielectric Elliptic Shell

A-K. Hamid

Department of Electrical and Computer Engineering
University of Sharjah
P.O. Box 27272, Sharjah, U.A.E
email: akhamid@Sharjah.ac.ae

Abstract **–** An analytic solution to the problem of scattering of a plane electromagnetic wave by a lossy or lossless dielectric confocal elliptic shell loading a semi-elliptic channel is derived. The incident, scattered and transmitted fields in every region are expressed in terms of complex Mathieu functions. Applying the boundary conditions at various faces and interfaces along with the partial orthogonality properties of angular Mathieu functions, the unknown scattered and transmitted field coefficients are obtained. The presented numerical results show a good agreement with the published data especially for the case of a lossless dielectric shell loading a semi-circular channel.

I. INTRODUCTION

The electromagnetic scattering from grooves, channels and cracks have been investigated by many researchers. The investigations have shown that when these structures are loaded with dielectric materials, the overall scattering patterns significantly change and thus it is important to obtain an analytic solution to predict the new scattering behavior of the target.

Lately, there have been many analytic studies available in the literature on the scattering by hollow and lossless dielectric loaded semi-circular or elliptic channels [1-9]. Most of these studies were based on the exact series eigen-function solution. On the other hand, numerical solutions based on the coupled integral equations for the induced currents were obtained by Senior et. al. [10-11].

To the best of our knowledge, there has been no analytical or numerical solution to the problem of scattering from a lossy or lossless dielectric elliptic shell loading a semi-elliptic channel in a ground plane.

In this paper, we present the solution to the scattering by a semi-elliptic channel loaded by two lossy dielectric layers. The presented solution will be the most general one available in the literature and the special lossless circular case may be deduced by making the axial ratios almost equal to unity [5], while the lossless dielectric coated conducting elliptic cylinder may be deduced by making the relative permittivity of the inside dielectric layer very high [9].

II. THEORY

Consider the case of a linearly polarized electromagnetic TM plane wave assumed to be incident on a lossy or lossless dielectric elliptic shell loading a semi-elliptic channel in a ground plane at an angle ϕ_i with respect to the x axis, as shown in Fig. 1. The major axis of the outer dielectric coating is denoted by a_2 and the minor axis is denoted by b_2. Furthermore, the major axis of inner dielectric elliptic cylinder is denoted by a_1 and the minor axis is denoted by b_1. The ground plane is assumed to be perfectly conducting.

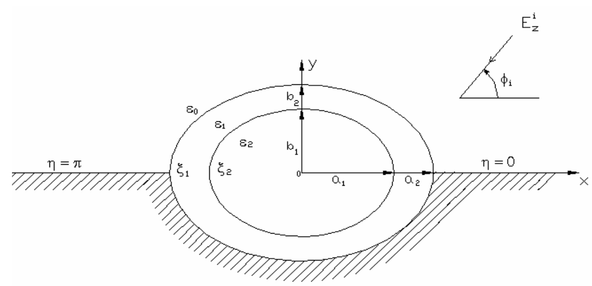

Fig. 1. Scattering geometry of a semi-elliptic channel in a ground plane loaded by a lossy or losslessconfocal dielectric elliptic shell.

The time dependence $e^{j\omega t}$ is assumed and omitted throughout. The elliptical coordinate system (u,v,z) is defined in terms of the Cartesian coordinate system (x,y,z) by $x = F\cosh(u)\cos(v)$ and $y = F\sinh(u)\sin(v)$, where F is the semi focal length of the elliptical cross section [12]. The electric field component of the TM polarized plane wave of amplitude E_0 is given in terms of polar coordinates ρ, ϕ by,

$$E_z^i = E_o e^{jk\rho\cos(\phi-\phi_i)} \tag{1}$$

where $k=2\pi/\lambda$ and λ is the wavelength. The incident electric field may be expressed in terms of Mathieu functions in elliptic cylindrical coordinates ξ, η as follows [12],

$$E_z^i = \sum_{m=0}^{\infty} A_{em}\,\mathrm{Re}_m^{(1)}(c_0,\xi)Se_m(c_0,\eta) + \sum_{m=1}^{\infty} A_{om}Ro_m^{(1)}(c_0,\xi)So_m(c_0,\eta) \quad (2)$$

$A_{\substack{em\\om}}$ and $N_{\substack{em\\om}}(c_o)$ are defined in [9], $c_O = kF$, Se_m and So_m are the even and odd angular Mathieu functions of order *m*, respectively, $\mathrm{Re}_m^{(1)}$ and $Ro_m^{(1)}$ are the even and odd radial Mathieu functions of the first kind of order *m*, while N_{em} and N_{om} are the even and odd normalized constants of order m. It should be noted that $\xi = \cosh u$ and $\eta = \cos v$ [12]. The reflected field ($\xi > \xi_1$ and $0 \le \eta \le \pi$) due to the presence of the ground plane can bewritten as,

$$E_z^{ref} = -\sum_{m=0}^{\infty} A_{em}\,\mathrm{Re}_m^{(1)}(c_0,\xi)Se_m(c_0,\eta) + \sum_{m=1}^{\infty} A_{om}Ro_m^{(1)}(c_0,\xi)So_m(c_0,\eta)\ . \quad (3)$$

The scattered field ($\xi > \xi_1$ and $0 \le \eta \le \pi$) due to the presence of the channel can be written as,

$$E_z^{diff} = \sum_{m=1}^{\infty} B_{om}Ro_m^{(4)}(c_0,\xi)So_m(c_0,\eta) \quad (4)$$

where B_{om} are the unknown odd scattered field expansion coefficients and $Ro_m^{(4)}$ is the odd radial Mathieu function of the fourth kind. The transmitted electric field inside the outer dielectric layer ($\xi_1 \le \xi \le \xi_2$) can also be written also in terms of Mathieu functions as,

$$E_z^I = \sum_{m=0}^{\infty}\begin{bmatrix} C_{em}\,\mathrm{Re}_m^{(1)}(c_1,\xi) \\ +D_{em}\,\mathrm{Re}_m^{(2)}(c_1,\xi)\end{bmatrix} Se_m(c_1,\eta) + \sum_{m=1}^{\infty}\begin{bmatrix} C_{om}Ro_m^{(1)}(c_1,\xi) \\ +D_{om}Ro_m^{(2)}(c_1,\xi)\end{bmatrix} So_m(c_1,\eta) \quad (5)$$

where $c_1 = k_1F$, $k_1 = k\sqrt{\varepsilon_{r1}}$, $\varepsilon_{r1} = \varepsilon_{r1}^{'} - j\varepsilon_{r1}^{''}$, C_{em}, D_{em} and C_{om}, D_{om} are the even and odd unknown tansmitted field expansion coefficients, and $\mathrm{Re}_m^{(2)}$ and $Ro_m^{(2)}$ are the even and odd radial Mathieu functions of the second kind [12]. Furthermore, the transmitted electric field inside the inner dielectric layer ($0 \le \xi \le \xi_2$) can also be expressed in terms of Mathieu functions as,

$$E_z^{II} = \sum_{m=0}^{\infty} G_{em}\,\mathrm{Re}_m^{(1)}(c_2,\xi)Se_m(c_2,\eta) + \sum_{m=1}^{\infty} G_{om}Ro_m^{(1)}(c_2,\xi)So_m(c_2,\eta) \quad (6)$$

where $c_2 = k_2F$, $k_2 = k\sqrt{\varepsilon_{r2}}$, $\varepsilon_{r2} = \varepsilon_{r2}^{'} - j\varepsilon_{r2}^{''}$ while G_{em} and G_{om} are the even and odd unknown transmitted field expansion coefficients. The magnetic field in every region can be obtained using Maxwell's equations. The unknown field expansion coefficients given in equations (4) to (6) are yet to be determined using the boundary conditions. The boundary conditions at $\xi = \xi_2$ require the tangential electric and magnetic field components in the inner and outer dielectric layers to be continuous. Enforcing this boundary condition along with orthogonality property of the angular Mathieu functions, we obtain

$$\sum_{m=0}^{\infty}\begin{bmatrix} C_{em}\,\mathrm{Re}_m^{(1)}(c_1,\xi_2) \\ +D_{em}\,\mathrm{Re}_m^{(2)}(c_1,\xi_2)\end{bmatrix} M_{emn}(c_1,c_2) = N_{en}(c_2)G_{en}\,\mathrm{Re}_n^{(1)}(c_2,\xi_2)\ , \quad (7)$$

$$\sum_{m=0}^{\infty}\begin{bmatrix} C_{em}\,\mathrm{Re}_m^{(1)'}(c_1,\xi_2) \\ +D_{em}\,\mathrm{Re}_m^{(2)'}(c_1,\xi_2)\end{bmatrix} M_{emn}(c_1,c_2) = N_{en}(c_2)G_{en}\,\mathrm{Re}_n^{(1)'}(c_2,\xi_2) \quad (8)$$

where

$$M_{\substack{emn\\omn}}(c_1,c_2) = \int_0^{2\pi} S_{om}^{em}(c_1,\eta)S_{on}^{en}(c_2,\eta)dv\ . \quad (9)$$

The prime in equation (8) denotes derivative with respect to u. Similar equations can be written corresponding to the odd solution. To eliminate G_{en}, we solve for G_{en} from equation (8) and substitute into equation (7). This leads to

$$\sum_{m=0}^{\infty} C_{em}\begin{Bmatrix} \mathrm{Re}_m^{(1)}(c_1,\xi_2) - \\ \mathrm{Re}_m^{(1)'}(c_1,\xi_2)u_{en}\end{Bmatrix} M_{emn}(c_1,c_2) + \sum_{m=0}^{\infty} D_{em}\begin{Bmatrix} \mathrm{Re}_m^{(2)}(c_1,\xi_2) - \\ \mathrm{Re}_m^{(2)'}(c_1,\xi_2)u_{en}\end{Bmatrix} M_{emn}(c_1,c_2) = 0\ . \quad (10)$$

We can write a similar equation for the odd solution, i.e,

$$\sum_{m=0}^{\infty} C_{om} \begin{Bmatrix} Ro_m^{(1)}(c_1,\xi_2) - \\ Ro_m^{(1)'}(c_1,\xi_2) u_{on} \end{Bmatrix} M_{omn}(c_1,c_2)$$
$$+ \tag{11}$$
$$\sum_{m=0}^{\infty} D_{om} \begin{Bmatrix} Ro_m^{(2)}(c_1,\xi_2) - \\ Ro_m^{(2)'}(c_1,\xi_2) u_{on} \end{Bmatrix} M_{omn}(c_1,c_2) = 0$$

where

$$u_{\substack{en \\ on}} = \frac{R_{on}^{en(1)}(c_2,\xi_2)}{R_{om}^{en(1)'}(c_2,\xi_2)} \tag{12}$$

The boundary condition at $\xi = \xi_1 (\pi < \eta < 2\pi)$ requires the tangential electric field component to vanish at surface, and the total tangential electric and magnetic field components to be continuous across the interface at $\xi = \xi_1$ $(0 < \eta < \pi)$. Enforcing these boundary conditions along with the partial orthogonality property of the angular Mathieu functions, we get [7, 9]

$$\sum_{m=0}^{\infty} \begin{bmatrix} C_{em} \,\mathrm{Re}_m^{(1)}(c_1,\xi_1) + \\ D_{em} \,\mathrm{Re}_m^{(2)}(c_1,\xi_1) \end{bmatrix} L_{mn} + \begin{bmatrix} C_{on} Ro_n^{(1)}(c_1,\xi_1) + \\ D_{on} Ro_n^{(2)}(c_1,\xi_1) \end{bmatrix} (\pi / 2.0) = 0.0, \tag{13}$$

$$\sum_{m=1}^{\infty} 2A_{om} Ro_m^{(1)}(c_0,\xi_1) W_{mn} + \sum_{m=1}^{\infty} B_{om} Ro_m^{(4)}(c_0,\xi_1) W_{mn} = \sum_{m=0}^{\infty} \begin{bmatrix} C_{em} \,\mathrm{Re}_m^{(1)}(c_1,\xi_1) + \\ D_{em} \,\mathrm{Re}_m^{(2)}(c_1,\xi_1) \end{bmatrix} F_{mn} + \begin{bmatrix} C_{on} Ro_n^{(1)}(c_1,\xi_1) + \\ D_{on} Ro_n^{(2)}(c_1,\xi_1) \end{bmatrix} (\pi / 2.0), \tag{14}$$

$$\sum_{m=1}^{\infty} 2A_{om} Ro_m^{(1)'}(c_0,\xi_1) W_{mn} + \sum_{m=1}^{\infty} B_{om} Ro_m^{(4)'}(c_0,\xi_1) W_{mn} = \sum_{m=0}^{\infty} \begin{bmatrix} C_{em} \,\mathrm{Re}_m^{(1)'}(c_1,\xi_1) + \\ D_{em} \,\mathrm{Re}_m^{(2)'}(c_1,\xi_1) \end{bmatrix} F_{mn} + \begin{bmatrix} C_{on} Ro_n^{(1)'}(c_1,\xi_1) + \\ D_{on} Ro_n^{(2)'}(c_1,\xi_1) \end{bmatrix} (\pi / 2.0) \tag{15}$$

where

$$W_{mn} = \int_0^{\pi} So_m(c_0,\eta) So_n(c_1,\eta) dv, \tag{16}$$

$$F_{mn} = \int_0^{\pi} Se_m(c_1,\eta) So_n(c_1,\eta) dv, \tag{17}$$

$$L_{mn} = \int_{\pi}^{2\pi} Se_m(c_1,\eta) So_n(c_1,\eta) dv = -F_{mn}. \tag{18}$$

Equations (13) to (15) are evaluated for m=0,1,2… and n=0,1,2,.... In case of $c_o=c_1$, equation (16) reduces to Wmn=$(\pi/2.0)\,\delta_{mn}$, where δ_{mn} is the Kronecker delta. Equations (10), (11), and (13) to (15) may be written in matrix form to solve for the unknown scattered and transmitted field expansion coefficients [9].

The lossy case requires the computation of Mathieu functions with complex argument and more details on the computation of Mathieu function can be found in [13-14].

III. NUMERICAL RESULTS

The scattered near and far fields can be calculated once the scattered field expansion coefficients are computed. The scattered far field expression may be written as follows,

$$E_z^s = \sqrt{\frac{j}{k\rho}} e^{-jk\rho} P(c_o,\eta) \tag{19}$$

where

$$P(c_o,\eta) = \sum_{m=1}^{\infty} j^m \left[B_{om} So_m(c_o,\eta) \right]. \tag{20}$$

In order to solve for the unknown scattered field coefficients, the infinite series are first truncated to include only the first *N* terms, where *N* in general is a suitable truncation number proportional to the channel electrical size. In the computation, the value of *N* has been chosen to impose a convergence condition that provides solution accuracy with at least four significant figures, The accuracy of the numerical results is checked against the special case of a semi-circular channel loaded with a lossless dielectric shell [4].

Figure 2 shows the normalized backscattered field $|P(c_o,\cos\phi_i)|$ for a lossy or lossless dielectric shell loading a semicircular channel versus ka_2 with ka_1=1.0, a_1/b_1=1.0, ε_{r1} = 1.5, ε_{r2} = 12 and ϕ_i = 90°. The solid line represents the calculated numerical results while the circled curve represents the solution in [4]. For example, the convergence for this is achieved for *N*=9. It can be seen that the calculated results agree very well with [4] for ka_2 < 3.2, the range given by [4]. Further, high peak resonances occur at different values of ka_2 and the amplitude of these peaks becomes even larger with the channel size. The strong resonant behavior may be due to the multiple scattering between the circular shell and channel. Finally, the dotted line represents the lossy dielectric case with ε_{r1} = 1.5- j0.5 and ε_{r2} = 12-j0.5. For example, the convergence for this is achieved for N = 7. The presence of lossy material seems to have little effect on the normalized backscattered field especially for ka_2 < 2.0, and attenuates the amplitude of the high peak resonances for ka_2 > 2.0. Figure 3 shows the normalized backscattered field for a lossy or lossless confocal dielectric elliptic shell loading a semi-elliptic channel versus the major axis of electrical size ka_2 . The major axis electrical size of the inner elliptic dielectric shell is kept constant at ka_1=1.0 with axial ratio a_1/b_1=1.43 and ϕ_i = 90^o. The solid line represents the lossless dielectric case, ε_{r1} = 3.0 and ε_{r2} = 5.0. The circled line represents the weakly lossy case, ε_{r1} = 3.0-j0.1 and ε_{r2} = 5.0-j0.1, while the dotted curve represents the strongly lossy case of ε_{r1} = 3.0-j0.5 and ε_{r2} = 5.0-j0.5.

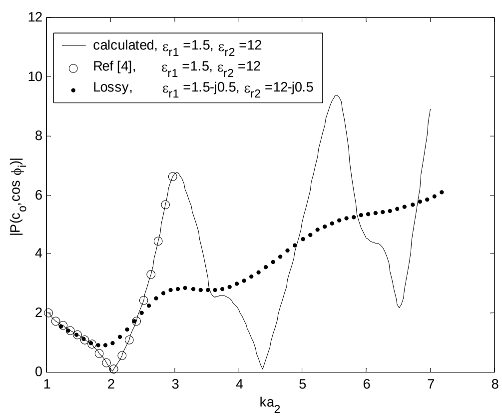

Fig. 2. Normalized backscattered field versus electrical size ka_2 for a lossy or lossless dielectric circular shell loading a semi-circular channel with ka_1=1.0, a_1/b_1=1.0 and ϕ_i = 90^o.

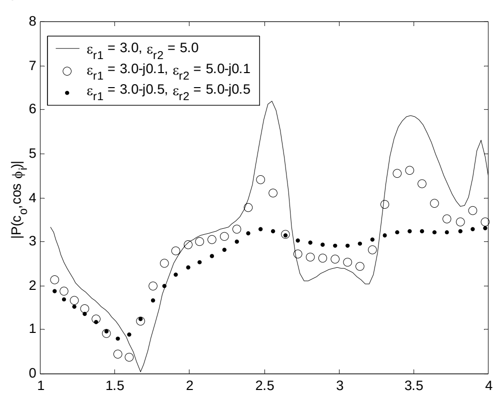

Fig. 3. Normalized backscattered field versus electrical size ka_2 for a lossy or lossless confocal dielectric elliptic shell loading a semi-elliptic channel with ka_1=1.0, a_1/b_1=1.43 and ϕ_i = 90^o.

In Fig. 4 we have plotted the normalized echo pattern width $|P(c_o, \cos\phi)|$ against the scattering angle ϕ for a lossy or lossless dielectric circular shell loading a semi-circular channel with ka_1=2.0, a_1/b_1=1.0, $ka_2=2\pi$, a_2/b_2=1.0 and ϕ_i =60^o. The solid line represents the lossless case with ε_{r1} = 4.0, ε_{r2} = 2.0. A strong resonance with high amplitude is located at ϕ =120^o, as expected, in addition to other resonances located at ϕ =40^o and 90^o. It seems that the presence of lossy dielectric material has little effect on the amplitude of the resonance at ϕ =120^o while strong effect may be observed on the amplitude of the resonances located at ϕ = 40^o and 90^o. Figure 5 shows normalized echo pattern width for a lossy or lossless dielectric elliptic shell loading a semi-elliptic channel with ka_1=5.73, a_1/b_1=5.73, $ka_2=2\pi$, a_2/b_2=2.3 and ϕ_i = 60^o. The solid line represents the lossless case, ε_{r1} = 4.0, ε_{r2} = 2.0, which seems to have strong resonances at different scattering angles and the strongest resonance peak is located at ϕ = 120^o. It can also be observed that the presence of the lossy dielectric material has a significant effect on the amplitude of the high peaks resonances, but has no effect on the location of resonances.

Figure 6 shows the normalized backscattered far field versus the incident angle ϕ_i for a lossy or lossless dielectric elliptic shell loading a semi-elliptic channel with ka_1=2.0, a_1/b_1=2.0, ka_2=4.36 and a_2/b_2=1.1. It seems that the normalized backscattered field of the elliptical channels is highest at the incident angle ϕ_i = 90^o. It can also be observed that the presence of lossy dielectric material has shifted the resonance peaks at ϕ_i = 30^o and 55^o.

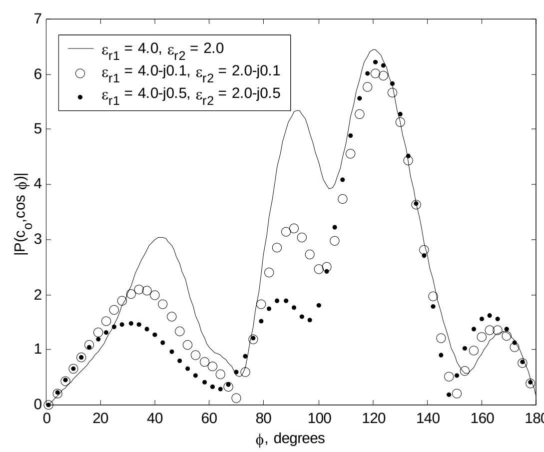

Fig. 4. Normalized scattered field versus the scattering angle ϕ for a lossy or lossless dielectric circular shell loading a semi-circular channel with ka_1=2.0, a_1/b_1=1.0, $ka_2 = 2\pi$, a_2/b_2 = 1.0 and ϕ_i = 60^o.

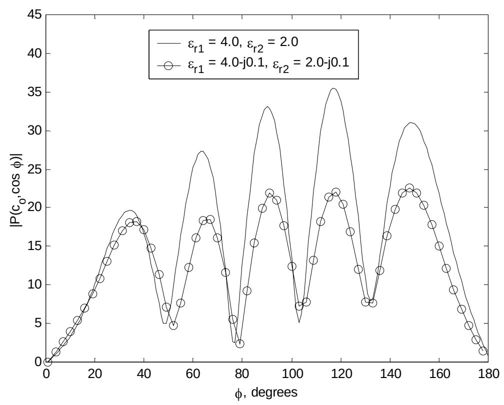

Fig. 5. Normalized scattered field versus the scattering angle ϕ for a lossy or lossless dielectric elliptic shell loading a semi-elliptic channel with ka_1 = 5.73, a_1/b_1 = 5.73, $ka_2 = 2\pi$, a_2/b_2 = 2.3 and $\phi_i = 60^o$.

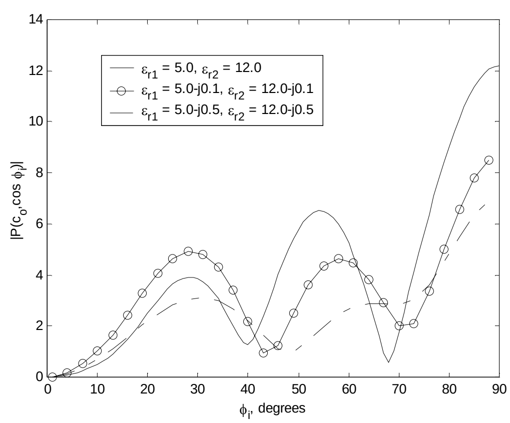

Fig. 6. Normalized backscattered field versus the incident angle ϕ_i for a lossy or lossless dielectric elliptic shell loading a semi-elliptic channel with ka_1 = 2.0, a_1/b_1 = 2.0, ka_2 = 4.36, a_2/b_2 = 1.1.

IV. CONCLUSIONS

An analytical solution and numerical results for the electromagnetic scattering by a lossy or lossless dielectric circular or elliptic shell loading a semi-circular or semi-elliptical channel in a ground plane is obtained. The presence of lossy or lossless dielectric shell has significantly affected the appearance and attenuation of the channel resonances. Finally, the presented solution is the most general one available in the literature and special cases can be deduced by choosing the appropriate axial ratio and dielectric constant.

ACKNOWLEDGEMENT

The author wishes to acknowledge the support provided by the University of Sharjah, U.A.E.

REFERENCES

[1] B. K. Sachdeva and R. A. Hurd, “Scattering by a dielectric-loaded trough in a conducting plane,” *J. Appl. Phys.*, vol. 48, no. 4, pp. 1473-1476, 1977.

[2] M. K. Hinders and A. D. Yaghjian, “Dual-series solution to scattering from a semicircular channel in a ground plane,” *IEEE Microwave Guided Wave Lett*., vol. 1, no. 9, pp. 239-242, 1991.

[3] T. J. Park, H. J. Eom, W.-M. Boerner, and Y. Yamaguchi, “TM scattering from a dielectric-loaded semi-circular trough in a conducting plane,” *IEICE Trans. Commun*., vol. E75-B, no. 2, pp. 87-91, 1992.

[4] T. J. Park, H. J. Eom, Y. Yamaguchi, W.-M. Boerner, and S. Kozaki, “TE-plane wave scattering from a dielectric-loaded semi-circular trough in a conducting plane,” *J. Electromagnetic Waves Applicat.*, vol. 7, pp. 235-245, 1993.

[5] H. A. Ragheb, “Electromagnetic scattering from a coaxial dielectric circular cylinder loading a semicircular gap in a ground plane,” *IEEE Trans. Microwave Theory Tech.*, vol. 43, no. 6, pp. 1303-1309, 1995.

[6] T. Shen, W. Dou, and Z. Sun, “Gaussian beam scattering from a semicircular channel in a conducting plane,” *Progress In Electromagnetics Research (PIER)*, vol. 16, pp. 67-85, 1997.

[7] W. J. Byun, J. W. Yu, and N. H. Myung, “TM scattering from hollow and dielectric –filled semielliptic channels with arbitrary eccentricity in a perfectly conducting plane,” *IEEE Trans. Microwave Theory Tech.*, vol. 46, no. 9, pp. 1336-1339, 1998.

[8] D. Erricolo and P. L. E. Uslenghi, “Exact radiation and scattering for an elliptic metal cylinder at the interface between isorefractive half-spaces” *IEEE Trans. on Antennas and Propag.*, vol. 52, no. 9, pp. 2214-2225, 2004.

[9] A-K. Hamid, “Electromagnetic scattering from a dielectric coated conducting elliptic cylinder loading a semi-elliptic channel in a ground plane,” *J. Electromagnetic Waves Applicat.*, vol. 19, no. 2, pp. 257-269, 2005.

[10] T. B. Senior and J. L. Volakis, "Scattering by gaps and cracks," *IEEE Trans. Antennas Propag.*, vol. 37, pp. 744-750, 1989.

[11] T. B. Senior, K. Sarabandi, and J. Natzke, "Scattering by a narrow gap," *IEEE Trans. Antennas Propag.*, vol. 38, pp. 1102-1110, 1990.

[12] P. M. Morse and H. Feshbach, *Methods of TtheoreticalPphysics*, vols. I and II. New York: McGraw-Hill, 1953.

[13] A-K. Hamid, M. I. Hussein, H. Ragheb, and M. Hamid, "Mathieu functions of complex arguments and their applications to the scattering by lossy elliptic cylinders," *Applied Computational Electromagnetics Society*, vol. 17, no. 3, pp. 209-217, 2002.

[14] A-K. Hamid and M. I. Hussein, "Electromagnetic scattering by a lossy dielectric coated elliptic cylinder," *Canadian Journal of Physics*, vol. 81, no. 5, pp. 771-778, 2003.

A.-K. Hamid was born in Tulkarm, West Bank, on Sept. 9, 1963. He received the B.Sc. degree in Electrical Engineering from West Virginia Tech, West Virginia, U.S.A. in 1985. He received the M.Sc. and Ph.D. degrees from the University of Manitoba, Winnipeg, Manitoba, Canada in 1988 and 1991, respectively, all in Electrical Engineering. From 1991-1993, he was with Quantic Laboratories Inc., Winnipeg, Manitoba, Canada, developing two and three dimensional electromagnetic field solvers using boundary integral method. From 1994-2000 he was with the faculty of electrical engineering at King Fahd University of Petroleum and Minerals, Dhahran, Saudi Arabia. Since Sept. 2000 he has been an associate Prof. in the electrical/electronics and computer engineering department at the University of Sharjah, Sharjah, United Arab Emirates. His research interest includes EM wave scattering from two and three dimensional bodies, propagation along waveguides with discontinuities, FDTD simulation of cellular phones, and inverse scattering using neural networks.